

Investigating interference between LoRa and IEEE 802.15.4g networks

Charalampos Orfanidis¹, Laura Marie Feeney¹, Martin Jacobsson^{1,2}, Per Gunningberg¹

¹Department of Information Technology, Uppsala University, Sweden

²School of Technology and Health, KTH, Sweden

{charalampos.orfanidis, lmfeeney, martin.jacobsson, per.gunningberg}@it.uu.se

Abstract—The rapid growth of new radio technologies for Smart City/Building/Home applications means that models of cross-technology interference are needed to inform the development of higher layer protocols and applications. We systematically investigate interference interactions between LoRa and IEEE 802.15.4g networks. Our results show that LoRa can obtain high packet reception rates, even in presence of strong IEEE 802.15.4g interference. IEEE 802.15.4g is also shown to have some resilience to LoRa interference. Both effects are highly dependent on the LoRa radio’s spreading factor and bandwidth configuration, as well as on the channelization. The results are shown to arise from the interaction between the two radios’ modulation schemes. The data have implications for the design and analysis of protocols for both radio technologies.

I. INTRODUCTION

We present a systematic measurement study of Cross-Technology Interference (CTI) between LoRa and IEEE 802.15.4g networks. Using controlled interference scenarios, we are able to quantify each network’s resilience to CTI and explain their behavior in terms of their respective modulation.

Both technologies use unlicensed spectrum that may be freely used by anyone, subject to regulatory constraints on transmit power and spectrum utilization. Operating in unlicensed spectrum is attractive because both network providers and individual users can deploy and use wireless devices without complex and costly administrative overhead. This flexibility has enabled the development of many applications that are becoming part of daily life. As a result, there are an increasing number of *independent* networks operating at the same location, using the same unlicensed spectrum and hence competing for transmission time. These networks are very diverse, with radios and communication protocols that are variously optimized for high data rates, long range, low power consumption, or high reliability.

Future smart building and smart city IoT applications will therefore need to be able to operate reliably in an environment where interfering networks use the shared spectrum in very different ways. Understanding and mitigating the impact of cross-technology interference among heterogeneous networks is therefore an important challenge.

LoRa (*Long Range*) [1] is a recently developed sub-GHz low-power wide-area network (LPWAN) technology. It uses a proprietary modulation to obtain high receiver sensitivity and achieve long-range, low-bitrate communication. One of its main use cases is as an infrastructure network providing

simple uplink capability for low power consumption devices. Another popular sub-GHz radio technology is IEEE 802.15.4g [2], an IEEE 802.15.4 [3] PHY layer developed in the context of Smart Utility Network applications [4]. It provides higher data rates and correspondingly shorter range than LPWAN solutions. Since both technologies are likely to be used simultaneously in urban areas, it is important to investigate the impact of their interference on each other.

Several papers have studied LoRa communication performance and scalability with respect to interactions within and between LoRa networks. To the best of our knowledge, this paper is the first to present a systematic measurement study of the interactions between LoRa and IEEE 802.15.4g networks operating in the EU 868 MHz unlicensed spectrum.

By creating highly controlled scenarios where transmitted packets are exposed to (almost) continuous interference, we are able to quantify the impact of interference on the Packet Reception Rate (PRR) in both networks. Our results show that LoRa is resilient enough to get high PRR even when the strength of an interfering IEEE 802.15.4g signal is considerable higher than the LoRa signal strength at the receiver. At moderate data rates, the LoRa PRR is almost unaffected by a 16 dB higher interference signal from IEEE 802.15.4g. Even at LoRa’s highest data rate settings it seems to tolerate up to 6 dBm of IEEE 802.15.4g interference.

IEEE 802.15.4g is more sensitive than LoRa to interference, but this depends very much also on the settings of the LoRa parameters, not only the power level since LoRa is sweeping over the IEEE 802.15.4g frequencies. We explain the interaction behaviors in terms of interference power, LoRa radio configuration parameters (notably the bandwidth and spreading factor), and the two radios’ modulation schemes.

Our contributions are useful for at least three purposes: First, our results can influence future work in cross-technology interference mitigation. Second, they can be used to parameterize and validate interference models and simulations. Finally, our work can inform future regulations on how to effectively share unlicensed spectrum.

The paper is organized as follows: Sections II and III describe the state of the art and provide background about these radio technologies. Section IV describes our methodology and presents the results and Section V concludes the paper.

II. RELATED WORK

There are numerous LPWAN technologies emerging. LoRa, in particular, has attracted both research and industry interest because of its long range and robust performance. Existing research mostly focuses on LoRa's performance, especially its transmission range, capacity, and scalability and on interaction between LoRa transmissions. They include [5–7], where the authors evaluate LoRa performance under various set of configurations and conditions. For instance, [5] introduces an algorithm for selecting proper parameters considering a desired energy consumption and link quality. In [7], a measurement study shows that vegetation has a big impact on LoRa transmissions. The Spreading Factor (SF) and the transmission data rate have a significant impact on the network coverage according to [6].

LoRa scalability is investigated in [8–10]. The authors in [8] analyze a LoRa network using a single gateway. Their results show that with an increase in the number of end-devices, the coverage probability drops exponentially, due to their interfering signals. In [9], simulation is used to show that multiple base stations improves the network performance under interference. In [10], the authors focus on the performance impact of LoRa on higher layers. Notably from their work is that the down-link receive window is seen as the limiting factor. This work, like the others, identifies that the main scalability limit of LoRa is its channel access protocol (essentially ALOHA) together with its rather expensive packet acknowledgements.

Finally, the work most closely related to ours is [11], an empirical study of interference between LoRa networks (a pre-print at the time of this writing). The paper investigates the interference case when one LoRa radio uses conventional LoRa modulation and the other one uses 2-GFSK modulation, which is also used in IEEE 802.15.4g. (Support for 2-GFSK is required in the LoRa specification.) The experiments use randomized packet lengths and inter-arrival times for both the sender and the interferer. The inter-arrival times are a significant fraction of (and in some cases longer than) the packet transmission times. This means that the proportion of time that the channel is interfered varies depending on the choice of LoRa transmission parameters. As a consequence, the results reflect a mix of heavily and minimally interfered packets. It is therefore hard to draw conclusions about the interference behavior, beyond the specific empirical observations. By contrast, we are doing much more controlled experiments that allow us to examine the interaction between the two modulations in detail.

III. BACKGROUND

In this section, we give the necessary background information about LoRa, IEEE 802.15.4g, and the spectrum overlap of these two wireless technologies.

A. LoRa

LoRa [1] uses a proprietary modulation scheme by the company Semtech based on Chirp Spread Spectrum (CSS), which

is both energy efficient and can achieve long distance transmissions. Chirp Spread Spectrum (CSS) is a spread spectrum technique, using wideband linear frequency modulated chirp pulses to represent information. A chirp is a sinusoidal signal whose frequency increases or decreases linearly over time. Information is encoded in the sequence of frequencies present in each chirp. The LoRa operating frequencies in Industrial, Scientific, and Medical radio band (ISM) are EU:868 MHz and 433 MHz, USA:915 MHz and 433 MHz. The bit rate, range, and resilience to interference are determined by the configuration parameters of LoRa, which are listed below.

Carrier Frequency: Carrier Frequency (CF) determines the central transmission frequency. The range for LoRa device we used, Semtech XRange SX1272 [12], is from 860 to 1020 MHz.

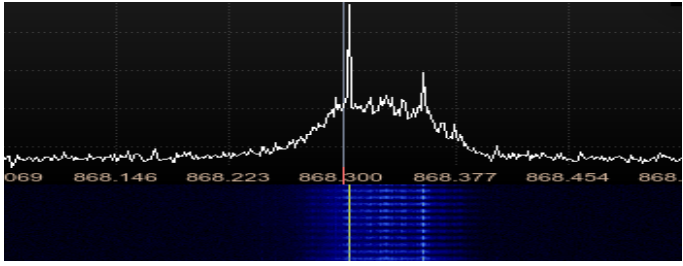
Bandwidth: The Bandwidth (BW) is the distance between the lowest and highest frequency in each chirp. A higher BW will increase the data rate and decrease the transmission time on air for a packet. It will also decrease the decoding sensitivity, since the radio signal is exposed more to noise. Using a low BW for the same size packet means longer transmission time and a higher risk that receiver will fall out of synchronization due to imperfect receiver clock drift. According to the specifications of the SX1272 modem, the available values for the BW are 125, 250 and 500 kHz.

Spreading Factor: Spreading Factor (SF) [13], is the ratio between the chip rate and the underlying symbol rate. If we increase the SF (i.e. more bits per symbol), the Signal to Noise Ratio (SNR) will be increased and consequently it will increase the range and the sensitivity, but also the time on air to send a symbol. The values available for this parameter are from 6 to 12 and the number of chips per symbol can be computed as 2^{SF} . For instance, with the value of 7 (SF7), we get 128 chips per symbol. Different SF can be used to separate transmission as they are orthogonal to each other.

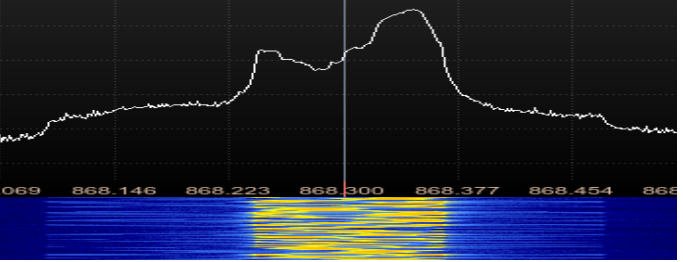
Coding Rate: LoRa uses Forward Error Correction (FEC) for the payload. The level of FEC is set by the Coding Rate (CR) parameter. CR increases robustness against interference but increases the time on air when more redundant bits are used for corrections.

B. IEEE 802.15.4g

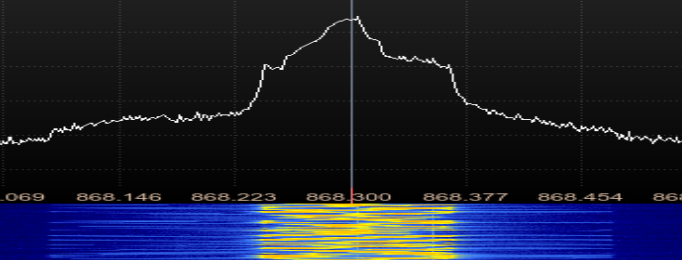
The IEEE 802.15.4 [3] is the standard for Low-Rate Wireless Networks. It operates in several different bands, including the popular 2.4 GHz band. Today, there is an increased usage in the sub-GHz bands. The IEEE 802.15.4 standard defines several different modulation schemes in the sub-GHz band. One important variant is the IEEE 802.15.4g (called SUN, Smart Utility Network, in the latest IEEE 802.15.4 standard), in the 863-870 MHz band, overlapping the LoRa frequencies. In this band, SUN uses up to 34 non-overlapping channels with 200 kHz spacing. SUN Mode # 1, achieves a data rate of 50 kbps using a bandwidth of 110 kHz with a frequency deviation of 50 kHz, which is the default configuration. SUN uses Frequency Shift Keying (FSK) or Gaussian Frequency Shift Keying (GFSK) modulation.



(a) IEEE 802.15.4g packet, output power 12 dBm at channel 26 (868.325 MHz). The channel is 200 kHz wide, with two sharp peaks separated by 50 kHz for the 2-GFSK modulation.



(b) LoRa packet with output power 12 dBm. The LoRa is configured for bandwidth 125 kHz and spreading factor SF12, centered at 868.3 MHz.



(c) IEEE 802.15.4g and LoRa packet collision, the LoRa packet overlaps the other packet.

Fig. 1: LoRa and IEEE 802.15.4g packet illustrated separately (1a, 1b) and when they collide (1c) captured by the Software Defined Radio (SDR). The vertical line shows the center capturing frequency for the SDR, which was 868.3 kHz.

C. Spectrum Overlap

Both LoRa and IEEE 802.15.4g (SUN) operate in the 868MHz license-free bands. There is both partial and complete overlap between the two technologies depending on the configurations of the two radios. We use 868.3 MHz as the LoRa center frequency, which allows us to use all three LoRa BWs. The overlap between LoRa and 802.15.4g standard is depicted in Fig. 6.

Fig. 1 presents the case when an IEEE 802.15.4g transmission collides with a LoRa transmission. In Fig. 1a, we see packet transmission from an IEEE 802.15.4g transmitter with 2-Level GFSK modulation with transmission power 12 dBm and in Fig. 1b, LoRa transmission with SF12, BW 125 kHz with transmission power 12 dBm. In Fig. 1c, LoRa completely overlaps the IEEE 802.15.4g packet as a superimposing of the transmissions. This is the main case we will investigate thoroughly in the next section of the paper.

IV. EXPERIMENTAL EVALUATION

This section describes our systematic measurement studies of the interaction between LoRa and IEEE 802.15.4g radios operating in 868 MHz spectrum. Details of the experimental setup are presented in section IV-A. We report on two groups of experiments: IEEE 802.15.4g communication subject to LoRa interference (section IV-B) and LoRa communication subject to IEEE 802.15.4g interference (section IV-C).

In each experiment, we measure the packet PRR between a transmitter and receiver in the presence of interfering transmissions from the other radio. Each radio occupies the channel as much as possible, maximizing collisions and allowing us to focus on low-level interactions between the two radios. To do this, we disabled the Channel Sensing and the MAC protocol on both the IEEE 802.15.4g and LoRa radios. Both the sender and the interferer were configured to transmit with a minimum gap between packets. This ensures that all packets experience interference over essentially their entire transmission time.

Our experiments were performed in an anechoic chamber, which is a radio isolated environment. This eliminates external interference and allows us to perform many hours of nearly continuous transmission, which spectrum regulations would otherwise make infeasible. The disadvantage of this approach is that the distances between radios are necessarily limited by the dimensions of the chamber. Our results therefore reflect relatively high signal strengths for both transmissions and interference. (Experiments using highly attenuated signals, operating closer to the limits of receiver sensitivity are deferred to future work.)

As we noted in Section III, LoRa and IEEE 802.15.4g have quite different channelization and modulation. In particular, there are two LoRa configuration parameters, SF and BW, that define timing patterns in the channel utilization. We therefore vary these parameters, along with the transmission power, to understand how these radios interfere with each other with respect to the parameters.

A. Experiment Setup

The LoRa radios are Semtech XRange SX1272 [12], equipped with a 3 dBi whip antenna. The host computer for the Semtech radio is Netblocks[14], running a variant of the lorablink [15] software, based on the freely available IBM/Semtech Lmic v1.6 [16] software. This software provides “bare-metal” access to the radio, allowing us fine-grain control of the transmission parameters and timing.

The LoRa packets contain a random payload of 59 B, an implicit header and a CRC checksum. The transmit time of the packet depends on the combination of LoRa parameters (SF, BW, CR) that are shown in Table I. The CR value we use is 4/5. The interval between packet transmissions is 576 μ sec, measured with an SDR [17] module.

The IEEE 802.15.4g radios are Texas Instruments CC1310 Launchpad [19], with a PCB antenna whose gain is 3.61 dBi. The nodes run Contiki OS [20]. The Contiki MAC and radio duty cycle are disabled to ensure minimum time gap between transmissions. Each IEEE 802.15.4g packet has a random

SF	CR 4/5			CR 4/8		
	BW125	BW250	BW500	BW125	BW250	BW500
7	108	54	27	160	80	40
8	195	98	49	287	144	72
9	340	175	87	509	254	127
10	657	329	162	952	476	238
12	2302	1151	575	3285	1642	821

TABLE I: Transmit time (ms) for a LoRa packet with 59 B payload for coding rates 4/5 and 4/8 (minimum and maximum redundancy, respectively). Each packet has an implicit header and a CRC checksum. Values from the Semtech LoRa Modem Calculator Tool [18].

payload of 106 B plus header and a CRC-16. The transmit time for each packet is a constant 21.18 msec and the interval between packets is 416 μ sec, measured with an SDR module.

As a result, all packets are exposed to interference from the other radio technology for essentially their entire duration. The LoRa packet transmit time is longer than the IEEE 802.15.4g packet transmit time. Each LoRa packet will therefore experience between one and sixty 416 μ sec gaps between interfering IEEE 802.15.4g transmissions. However, the interfering IEEE 802.15.4g transmissions still occupy the channel over 98% of the time.

Conversely, an IEEE 802.15.4g packet will experience at most one gap between interfering LoRa transmissions. This gap is 576 μ sec long, so an IEEE 802.15.4g packet will experience interference for at least 97% of its 21.18 msec transmit time.

We therefore consider packets as being continuously interfered in our analysis. In addition, we collect a sample of at least 100 interfered packets in each configuration. This ensures that any gaps in the interference occur at different times during packet transmission. In particular, the synchronization header is not specifically targeted or avoided with interference. This approach allows us to avoid requiring tight synchronization between the two radios to create interference scenarios.

output	LoRa interference power measured (dBm)			IEEE 802.15.4g TX power measured (dBm)
	BW 125	BW 250	BW 500	
12	-36	-36	-36	-51
10	-38	-39	-37	-52
8	-40	-40	-40	-53
6	-42	-42	-42	-56
4	-44	-44	-44	-58
2	-45	-48	-45	-61

TABLE II: TX power setting of the LoRa interferer, 802.15.4g transmitter and the resulting interference power and transmitting power measured at the IEEE 802.15.4g receiver.

B. LoRa interfering on IEEE 802.15.4g communication

Our first set of experiments examines how LoRa interference affects IEEE 802.15.4g communication. The IEEE 802.15.4g sender and receiver are placed 6.4 m apart in an anechoic chamber, 80 cm above the inner floor of the chamber. The LoRa interferer is placed 10.5 m away from the receiver. All nodes are in line-of-sight (Fig. 3a) and the printed circuit

board antennas on the IEEE 802.15.4g nodes are directed to face each other.

Table II shows the average received power measured at the position of the 802.15.4g receiver, for various output power settings at the 802.15.4g sender and again for the same output power settings at the LoRa interferer. The measurements were made manually, using a Keithley 2810 vector signal analyzer equipped with a 3 dBi whip antenna. The uncertainty is approximately ± 1 dBm. The PCB antenna on the IEEE 802.15.4 receiver has a different gain than the antenna on the signal analyzer, so the measured power is not exactly the same as the power received by the IEEE 802.15.4 radio. However, since both the interference and transmission power are measured using the same antenna (whether it is the signal analyzer or the IEEE 802.15.4 receiver) in each case, the ratio between the two power levels will be the same. The differences between the received and interfering powers obtained in this experiment layout range from -6dB to -24dB. As expected, the measured LoRa interference power does not depend on the BW parameter.

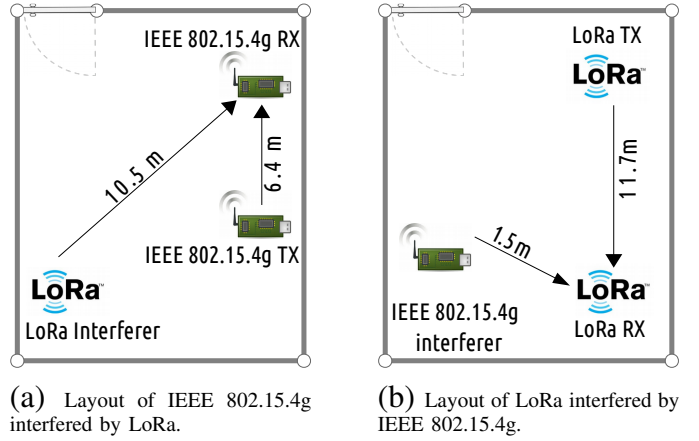


Fig. 3: Node deployment in the anechoic chamber.

1) *Packet Reception Rate under LoRa interference:* From our previous discussion, we expect that the PRR of IEEE 802.15.4g will vary with the relative received power from the two radios. A high BW of LoRa will affect more than one IEEE 802.15.4g channel and the SF of LoRa will be insignificant since it is intended to change the LoRa effective data rate without changing the BW or overall power.

Our PRR measurement results are presented in Fig. 2 as sets of "heatmap blocks". Each set of blocks represents one combination of BW and SF values. Each block represents a different IEEE 802.15.4g transmission power level, from 2 to 12 dBm. Within each block, the PRR "heat" level is illustrated with different blue colors, from white for zero received packets up to dark blue for 100% correctly received packets. The PRR color is given for IEEE 802.15.4g packets sent using each of five IEEE 802.15.4g channels, 24 to 28, marked on the x-axis in each block. For each block the LoRa interference power is varied from 2 to 10 dBm, given on the y-axis. The strength of the LoRa interferer relative to the IEEE 802.15.4g

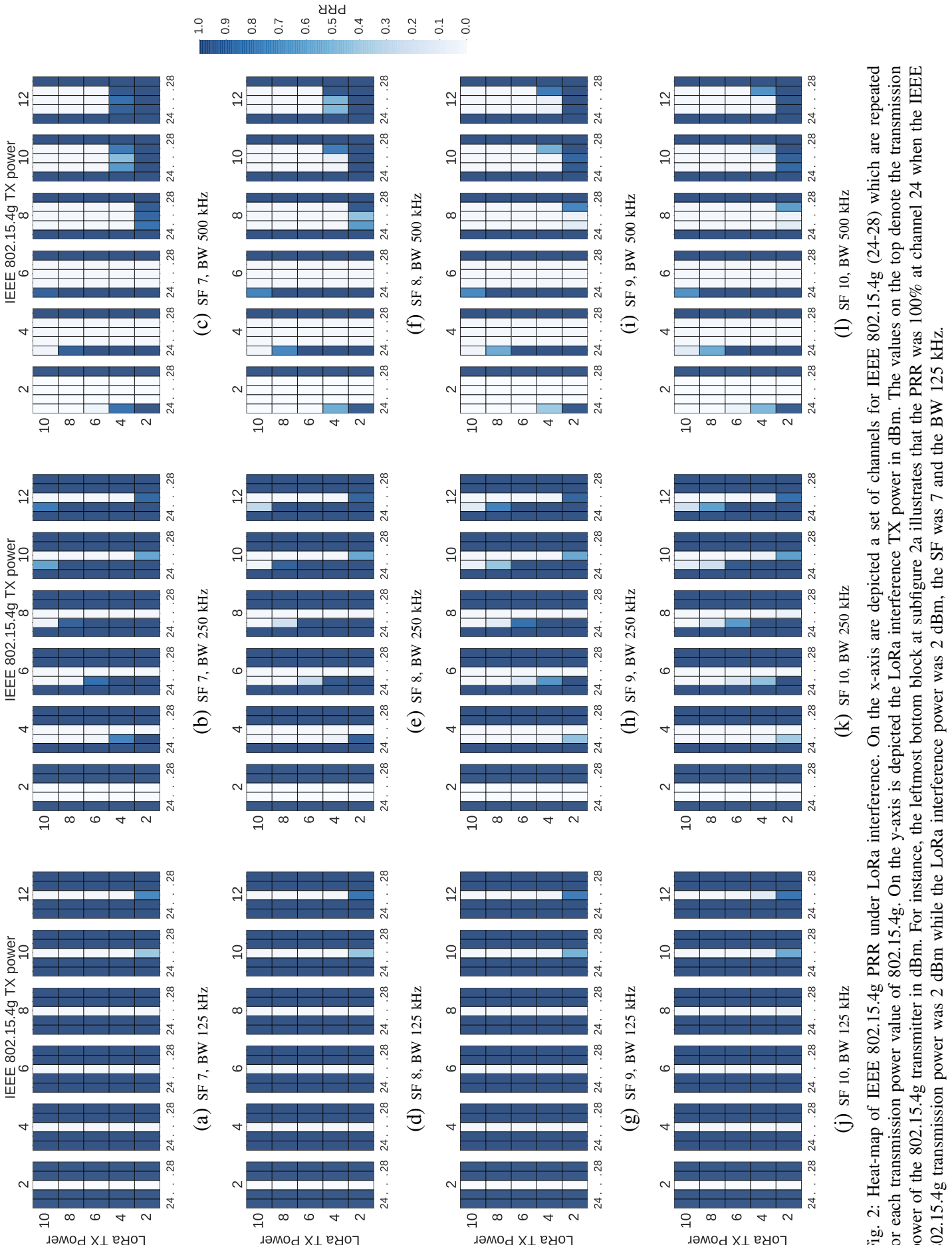


Fig. 2: Heat-map of IEEE 802.15.4g PRR under LoRa interference. On the x-axis are depicted a set of channels for IEEE 802.15.4g (24-28) which are repeated for each transmission power value of 802.15.4g. On the y-axis is depicted the LoRa interference TX power in dBm. The values on the top denote the transmission power of the 802.15.4g transmitter in dBm. For instance, the leftmost bottom block at subfigure 2a illustrates that the PRR was 100% at channel 24 when the IEEE 802.15.4g transmission power was 2 dBm while the LoRa interference power was 7 and the BW 125 kHz.

packet transmission can be inferred from the received power measurements in Table II. The frequencies used by the IEEE 802.15.4g sender and the LoRa interferer are shown in Fig. 6.

Starting with the leftmost sub-block in Fig. 2a, we see that LoRa severely interferes with channel 26 of IEEE 802.15.4g. The measured PRR on that channel became very close to zero, even at low LoRa power levels. The BW of LoRa is 125 kHz, which means that the interference band is confined to channel 26. The other channels around 26 are unaffected and consequently the measurements reached the highest PRR level, independent of the LoRa output power level. As the IEEE 802.15.4g transmit power increases (the rightmost sub-blocks in Fig. 2a), some packets are successfully received on channel 26, for the lowest levels of LoRa interference. The PRR becomes non-negligible once the LoRa interference is no more than 6-7dB higher than the received power.

Measurements with the LoRa BW set to 250 and 500 kHz respectively are reported in Figs. 2b-2c. As expected, LoRa's now larger band will interfere up to four IEEE 802.15.4g channels for the 500 kHz case (each channel is 200 kHz wide). The overall PRR pattern is though similar to the 125 kHz case but now the LoRa power is spread over more channels. Thus, for the stronger IEEE 802.15.4g power settings some higher PRR is achieved compared to the 125 kHz case.

The SF factor values used are 7 to 10 in Fig. 2. When comparing the PRR for different SF over the 125, 250 and 500 kHz cases respectively we see similar PRR patterns for each bandwidth which confirms our general hypothesis that the SF parameter has a relative small impact on the IEEE 802.15.4g transmission. The details and actual interactions will be further discussed below.

2) Discussion of the BW impact: With the LoRa center frequency set to 868.3 MHz, LoRa's 125 kHz BW interferes with a substantial portion of the 200 kHz wide IEEE 802.15.4g channel 26 (Fig. 6), resulting in substantial packet loss on that channel. When the LoRa BW is 250 kHz, a portion of IEEE 802.15.4g channel 25 also experiences interference. Some IEEE 802.15.4g packets sent on this channel are successfully received once the LoRa interference is no more than around 12-14dB higher than the received power, depending also on the SF (see below). When the BW is 500 kHz, up to four IEEE 802.15.4 channels are affected. Again, the channels experiencing the largest overlap suffer the most.

output	LoRa TX power measured (dBm)			IEEE 802.15.4g interference power measured (dBm)
	BW 125	BW 250	BW 500	
12	-34	-35	-36	-29
10	-36	-38	-37	-31
8	-38	-39	-40	-31
6	-41	-41	-42	-34
4	-43	-43	-44	-36
2	-44	-45	-45	-40

TABLE III: TX power setting of the LoRa sender, IEEE 802.15.4g interferer and the resulting transmitting and interference power measured at the LoRa receiver.

3) Discussion of the power impact: When the transmission power at IEEE 802.15.4g transmitter is increased, some packets are successfully received. For instance, if we compare the min and max output power for IEEE 802.15.4g in Fig. 2a when LoRa is interfering at 2 dBm the PRR goes from 0% to 74%. The interference level for that case is 6 dB high, even though some packets from the IEEE 802.15.4g transmitter are successfully received. This happens because LoRa uses CSS modulation, which means that the transmitted signals are chirps, which change frequency continuously in order to represent the requested symbol. On the other hand IEEE 802.15.4g uses 2-Level GFSK modulation which uses two different frequencies to transmit 0 or 1. When the chirp is not completely at the same frequency with the GFSK signal and the power in GFSK is strong enough, the packets are successfully received and not affected from the interference.

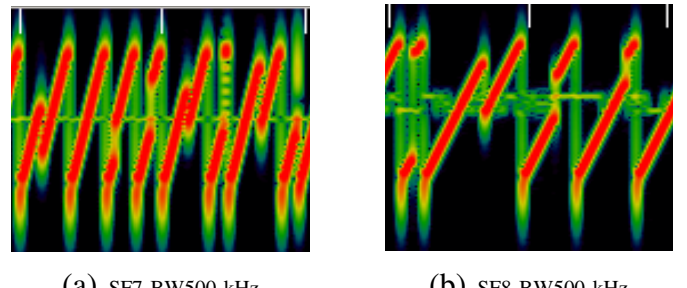


Fig. 4: Illustration of how the angle of the chirp changes when we change the SF in LoRa captured from the SDR. Time is along x-axis and frequency in y-axis.

4) Discussion of the SF impact: The PRR in IEEE 802.15.4g also decreases slightly with increasing SF in the LoRa interference. This is noticeable for BW 250 kHz and especially BW 500 kHz (Figs. 2c, 2f, 2i and 2l). An explanation of this behaviour is that when the SF increases, the angle of the chirp becomes shallower and overlaps more with the GFSK signal. Fig. 4 shows the angle difference of SF7 and SF8 chirps. With a larger SF, the degree of tolerance from IEEE 802.15.4g decreases because the two signals overlap more. Fig. 2c shows that when the difference between the interference power to transmission power is 7 dB and the SF is 7, the PRR is around 90% for channels 25-27. For the same configuration, but an SF of 10, Fig. 2l shows that two of the three interfered channels have 0% PRR and channel 27 drops to 73% PRR.

C. IEEE 802.15.4g interfering on LoRa communication

The second set of experiments examines how IEEE 802.15.4g interference affects LoRa communication. The LoRa transmitter and receiver are placed 11.7 m apart in an anechoic chamber, 80 cm above the inner surface of the chamber. The IEEE 802.15.4g interferer is 1.5 m away from the LoRa receiver and its printed circuit antenna is directed toward the LoRa receiver. All nodes are in line-of-sight (Fig. 3b).

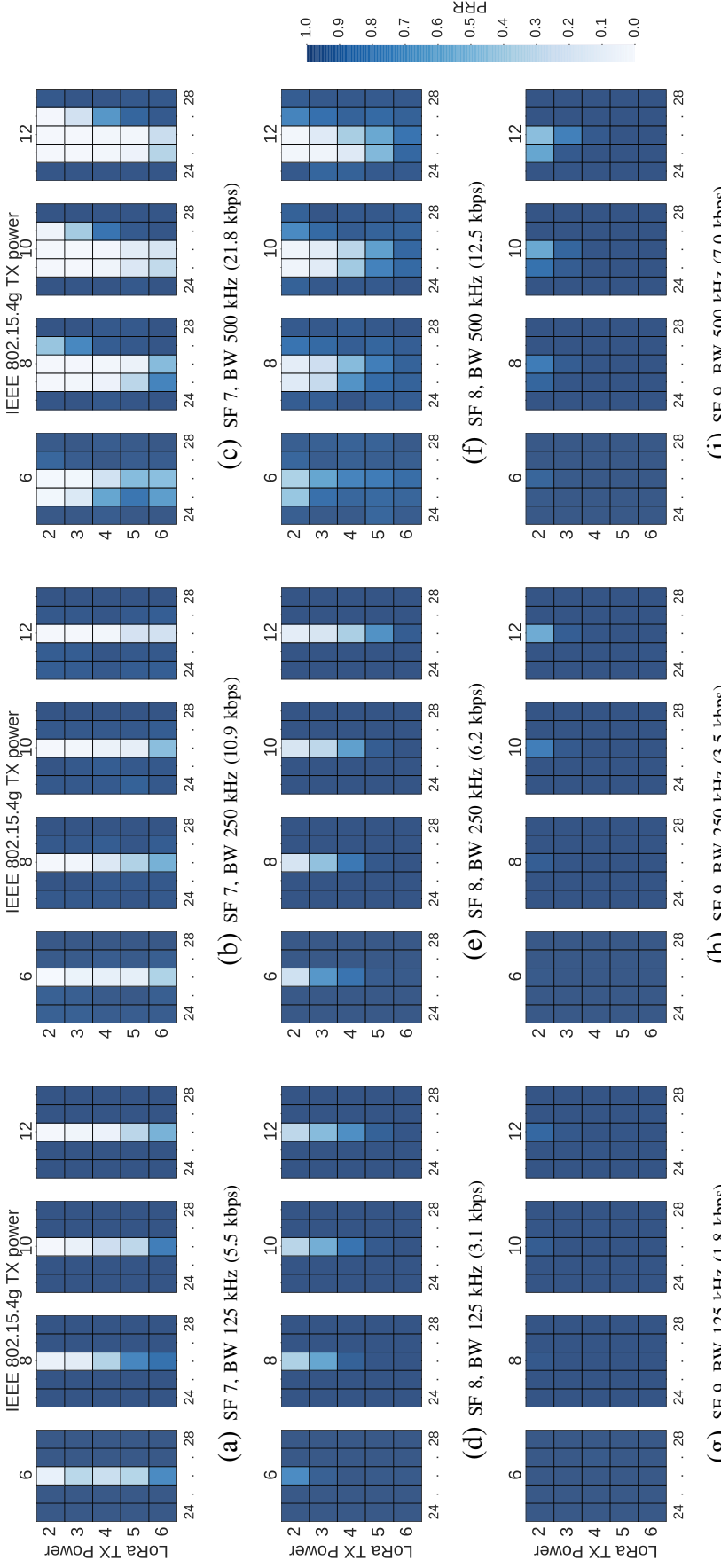


Fig. 5: Heat-map of LoRa PRR under IEEE 802.15.4g interference. The figure is similar to Figure 2, but now the IEEE 802.15.4g power and channels (x-axes) reflect the interference and the LoRa power (y-axes) reflects the interfered packets. The LoRa data rate doubles (left to right) as the bandwidth doubles and decreases by about half for each increase in spreading factor (top to bottom). In the lower left of each figure (LoRa TX power 6 dBm, IEEE 802.15.4g TX power 12 dBm), the interfering signal is about 7 dB higher at the receiver. In the upper right of each subfigure (LoRa TX power 2 dBm, IEEE 802.15.4g TX power 12 dBm), the interference is about 16 dB higher.

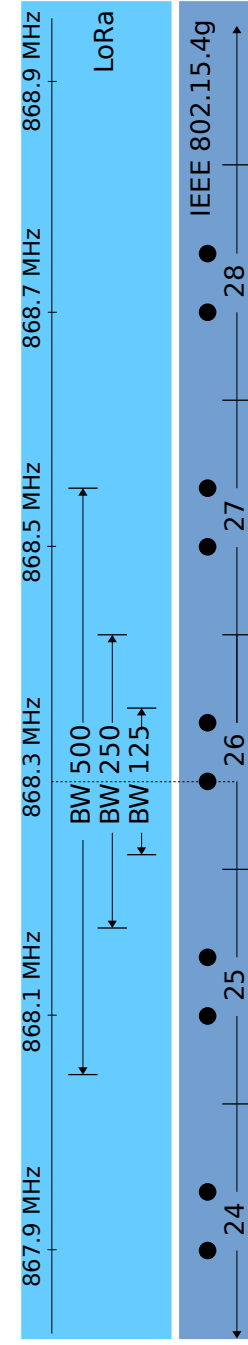


Fig. 6: 868 MHz unlicensed spectrum. LoRa (above) is configured to operate at a 868.3 MHz center frequency. The 3 BWs are shown. The IEEE 802.15.4g standard defines fixed channels (below). The channel spacing and the 2-GFSK frequency deviation (solid dots) are shown for each channel. The output power is highest at these two points (corresponding to the peaks in Figure 1a).

Table III is the analog of Table II. It shows the average power received at the position of the LoRa receiver, for various output power settings at the LoRa sender. Table III also shows the received power of the interfering IEEE 802.15.4g transmissions at the position of the LoRa receiver. The measurements were made manually using a Keithley 2810 vector signal analyzer; the uncertainty is approximately ± 1.5 dBm.

1) Packet Reception Rate under IEEE 802.15.4g interference: Fig. 5 presents a set of PRR heatmaps similar to those in Fig. 2. Each of the subfigures represents a LoRa radio configuration (SF and BW). Within each subfigure, each block represents a transmission power level of the IEEE 802.15.4g interferer. The same power is used on all channels 24 to 28, represented on the x-axis. The LoRa transmit power levels are given on the y-axis. The "blue heat color" of each small sub-block shows the PRR, i.e. the proportion of correctly received LoRa packets, for a given LoRa output power and IEEE 802.15.4g interference power and channel.

LoRa packets are – as expected – significantly more resilient to interference than IEEE 802.15.4g packets. For spreading factor SF9 and above, packet losses become negligible, even when the interferer is ~ 16 dB stronger according to the difference between LoRa and IEEE 802.15.4g interference power in Table III. Even at lower spreading factors and bandwidths, LoRa still obtains acceptable PRR when the interferer is 6 dB stronger.

2) Discussion of the LoRa PRR results: To some extent, the LoRa resilience can be explained by trading lower data rates against redundancy using higher spreading factors. This is in contrast to the experiment in the previous section, where the IEEE 802.15.4g packets have a fixed 50 kbps data rate.

The trade-off becomes visible when comparing the PRR for LoRa configurations with similar data rates but with different BW and SF factors, see Figs. 5i and 5e, or 5f and 5b. LoRa is more vulnerable to interference when using low bandwidth combined with a small spread factor.

Another contributing factor to the LoRa resilience is its modulation. LoRa uses CSS modulation in contrast to GFSK used by IEEE 802.15.4g. CSS spreads the energy of the symbol across the whole bandwidth while GFSK concentrates the energy to two shift frequencies making 802.15.4g more sensitive to narrowband interference. Their spread can be seen in Fig. 1a and Fig. 6.

V. CONCLUSION

We have evaluated the impact of cross-technology radio interference between LoRa and IEEE 802.15.4g networks with real experiments focusing on the PRR metric. In general, we conclude that LoRa is much more tolerant than IEEE 802.15.4g under interference and LoRa's radio configuration (SF and BW) are important to the degree of tolerance. At a high data rate setting, LoRa can tolerate interference power that is 6 dB higher than the actual LoRa receiving power and for the low data rate it can tolerate up to 16 dB with acceptable PRR. IEEE 802.15.4g seems to be resilient to LoRa

interference under some certain configurations of LoRa. More specific, IEEE 802.15.4g has some tolerance to LoRa which is depending on the parameters SF and BW. The significance of the results comes from the fact that they give insights in both radio platforms, which could help designing collision avoidance mechanisms and provide reliability and robustness to the higher layers. Such designs we leave for further work.

ACKNOWLEDGEMENT

This work has partly been carried out within the Swedish strategic innovation program on Internet of Things, which is a joint effort between VINNOVA, Formas, and the Swedish Energy Agency. We thank our colleagues from CoRe and UNO groups and Magnus Jobs of Department of Physics and Astronomy, Uppsala University for their help. We would also like to thank Martin Bor of Lancaster University for his help.

REFERENCES

- [1] LoRa Alliance, <https://www.lora-alliance.org>, Accessed 20.05.2017.
- [2] IEEE, "IEEE Standard for Local and Metropolitan Area Networks," *IEEE Std 802.15.4-2012 (Part 15.4: Low-Rate Wireless Personal Area Networks (LR-WPANs) Amendment 3: Physical Layer (PHY) Specifications for Low-Data-Rate, Wireless, Smart Metering Utility Networks)*, 2012.
- [3] ———, "IEEE standard for low-rate wireless networks," *IEEE Std 802.15.4-2015 (Revision of IEEE Std 802.15.4-2011)*, April 2016.
- [4] Wi-SUN Alliance, <https://www.wi-sun.org>, Accessed 20.05.2017.
- [5] M. Bor and U. Roedig, "LoRa transmission parameter selection," in *Proceedings of the 2017 International Conference on Distributed Computing in Sensor Systems*, ser. DCOSS, 2017, (Preprint).
- [6] A. Augustin, J. Yi, T. Clausen, and W. M. Townsley, "A study of LoRa: Long range & low power networks for the Internet of Things," *Sensors*, vol. 16, no. 9, 2016.
- [7] O. Iova, A. L. Murphy, G. P. Picco, L. Ghiro, D. Molteni, F. Ossi, and F. Cagnacci, "LoRa from the city to the mountains: Exploration of hardware and environmental factors," in *Proceedings of the 2017 International Conference on Embedded Wireless Systems and Networks*, ser. EWSN, 2017.
- [8] O. Georgiou and U. Raza, "Low power wide area network analysis: Can LoRa scale?" *IEEE Wireless Communications Letters*, vol. 6, no. 2, pp. 162–165, April 2017.
- [9] T. Voigt, M. Bor, U. Roedig, and J. Alonso, "Mitigating inter-network interference in LoRa networks," in *Proceedings of the 2017 International Conference on Embedded Wireless Systems and Networks*, ser. EWSN, 2017.
- [10] F. Adelantado, X. Vilajosana, P. Tuset-Peiro, B. Martinez, and J. Melia, "Understanding the limits of LoRaWAN," *arXiv preprint arXiv:1607.08011*, 2016.
- [11] K. Mikhaylov, J. Petäjäjärvi, and J. Janhunen, "On LoRaWAN scalability: Empirical evaluation of susceptibility to inter-network interference," *arXiv preprint arXiv:1704.04257*, 2017.
- [12] Semtech, <http://www.semtech.com/images/datasheet/sx1272.pdf>, Accessed 20.05.2017.
- [13] Semtech, <http://www.semtech.com/images/datasheet/an1200.22.pdf>, Accessed 13.06.2017.
- [14] Netblocks, <https://www.netblocks.eu/xrange-sx1272-lora-datasheet>, Accessed 20.05.2017.
- [15] M. Bor, J. Vidler, and U. Roedig, "LoRa for the Internet of Things," in *Proceedings of the 2016 International Conference on Embedded Wireless Systems and Networks*, ser. EWSN, 2016.
- [16] IBM Research, <https://www.research.ibm.com/labs/zurich/ics/lrsc/lmic.html>, Accessed 20.05.2017.
- [17] E. B210, https://www.ettus.com/content/files/b200-b210_spec_sheet.pdf, Accessed 20.05.2017.
- [18] Semtech, <http://www.semtech.com/>, Accessed 20.05.2017.
- [19] Texas Instruments, <http://www.ti.com/lit/ds/symlink/cc1310.pdf>, Accessed 20.05.2017.
- [20] Contiki OS, <http://www.contiki-os.org>, Accessed 20.05.2017.